

DESIGN, ANALYSIS AND 3D PRINTING OF AN UNMANNED AIRCRAFT WITH UNCONVENTIONAL STRUCTURE

Dana Cojocaru¹, Sebastian-Marian Zaharia²

¹Transilvania University of Brasov, dana.cojocaru@student.unitbv.ro

²Transilvania University of Brasov, zaharia_sebastian@unitbv.ro

ABSTRACT: Additive manufacturing (AM), also known as 3D printing, is a manufacturing process that produces three-dimensional products with complex geometries and shapes by depositing material. In this paper the aim was to manufacture an aircraft with an unconventional structure using additive manufacturing processes. The first step was the design of the UAV structural solution, for which CFD (Computational Fluid Dynamics) and FEM (Finite Element Analysis) analyses were carried out in order to validate the model. The second step that is the actual manufacture of the aircraft, the thermoplastic filament extrusion manufacturing process was used to obtain the components of the UAV model. The application of the thermoplastic extrusion process improved the aerodynamic characteristics and the strength of the aircraft, which was demonstrated by ground testing of the aircraft.

KEYWORDS: design, aerodynamic analysis, 3D printing, unconventional UAV structure, FEA.

1. INTRODUCTION

The importance of unmanned aerial vehicles (UAVs) can be seen in their widespread use in various areas where small, low-cost aircraft are needed but with a high degree of safety for those using them. These aircraft are very advantageous in terms of size and relatively small mass depending on the materials used and their manufacture, which makes them an object of interest for study, realization and use in various academic research institutions and economic activities [1].

UAVs can be classified according to size, configuration, empty weight, maximum take-off weight, operational altitude and speed [2]. UAVs have applications in various fields such as: industry, transportation, agriculture, surveying and geodesy, hydrography, medicine, environmental protection, critical infrastructure security, military [3]. It can be mentioned that now, aircraft with conventional structures prevail in terms of numbers, but there is continuous research of various structural solutions that can contribute to improve the performance, endurance, safety level and unconventional structure aircraft [4]. The technological evolution of aircraft manufacturing is very dynamic. In this context, it can be mentioned that additive processes are intensively used to manufacture parts for aircraft, and, more recently, for whole aircraft [5].

In the field of UAV manufacturing, this process is starting to be used more and more often, in contrast to classical manufacturing methods due to geometrical flexibility. Thus, the use of this process is very advantageous in the manufacturing of aircraft

with complex geometries or unconventional structures [1,5]. In this paper, the Fused Filament Fabrication (FFF) thermoplastic extrusion process was studied. This type of process consists of extruding an object by depositing a filament layer by layer through a nozzle. The filament is a wire of varying thickness, made from a material that meets the requirements for plastic melt [6,7].

As previously written, a considerable number of UAVs are relatively small in size, with a maximum wingspan of 2-3 m. Generally, the weight of the same model aircraft can vary depending on the material chosen, and in aviation the aim is to reduce it. Also, given the dimensions, the manufacturing process chosen is one that allows for small parts to be designed while still being of good quality.

The UAV that has been manufactured in this study is a twin-boom fuselage model which is an aircraft with an unconventional structure, for which the wings are fixed on the fuselage and two beams are fixed on the wings which act as tail, the surfaces of the empennage have been placed at the end of the two beams. Twin-tail aircraft have the following advantages: mounting a pusher propeller instead of a drag propeller; improved aerodynamics in the case of twin-engine aircraft or increased structural stiffness and increased volume inside [8].

2. UNMANNED AIRCRAFT DESIGN

Based on the analysis of several profiles in the XFLR5 software system, the NACA 4412 profile was chosen for the wing design. This airfoil showed the best lift and drag results for the required conditions. Thus, the wing for this aircraft has an

elliptical shape with a span of 1000 mm, fitted with 2 tubes embedded in the thickness of the profile to fix the rods to support the empennage (Figure 1). Inside the wing there are ribs arranged at 45°, with a distance of 40 mm between them, with lightening holes and a cut-out area for a 10 mm diameter cylindrical spar. The control surface is of rectangular shape which is cut out of the wing at a distance of 176 mm from the axis of symmetry of the wing.

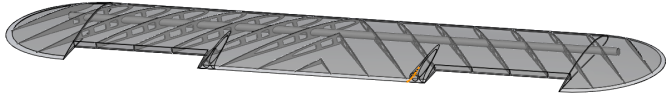


Figure 1. Wing structure

The empennage is made in the shape of an inverted V with a height of 153 mm and a width of 382 mm, thus forming an angle of approximately 53 degrees with the plane of longitudinal symmetry of the empennage (Figure 2).



Figure 2. Inverted V-shaped vertical empennage

The profile used to design the empennage is a symmetrical one, namely NACA 0018. The 2 parts of the empennage are joined at the upper edges by a 10 mm radius joint with cut-outs for the control surfaces. At the lower ends 2 tubes (Figure 3) are made for fixing to the rods which help to secure the empennage to the wing, and inside the empennage there are ribs arranged at 45 degrees and 40 mm from each other.

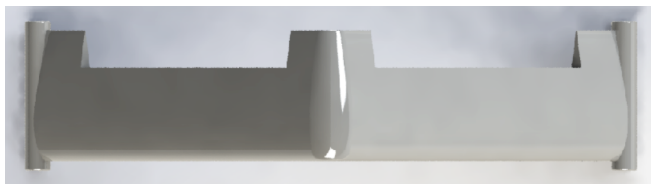


Figure 3. Horizontal stabilizer

The fuselage for this radio-controlled aircraft is aerodynamically shaped and has a cut-out area where the wing will be attached (Figure 4).

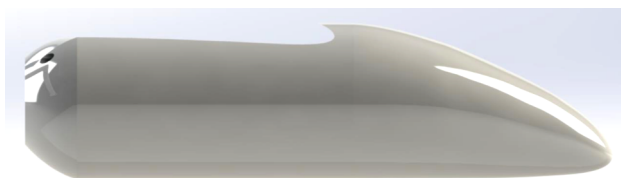


Figure 4. Fuselage structure

In the design of the UAV model, elements such as the landing gear, wheels, propeller, connecting rods for the empennage and wing were included. The best structural solution for this UAV was that the landing gear (Figure 5) was located at the rear, closer to the centre of gravity.

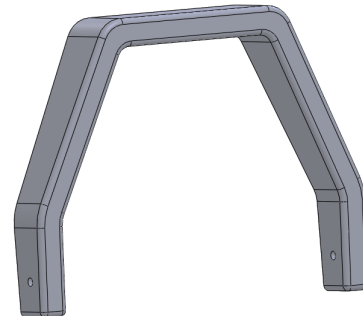


Figure 5. Main landing gear

Figure 6 shows the digital model, designed in the SolidWorks 2020 software system of the aircraft.



Figure 6. Digital model of the UAV

During the flight mission the aircraft performs the pre-defined operation. The aircraft is equipped with a video camera and during the mission it is possible to: monitor a specific area; collect images or video during the flight, which can be used for different flight missions. Table 1 shows the main characteristics of the 3D printed aircraft.

Table 1. Dimensional characteristics of the aircraft

Nr.	Characteristic	Value
1	Wingspan	1000 mm
2	Height	355 mm
3	Length	620 mm
4	Airfoil wing	NACA 4412
5	Airfoil empennage	NACA 0018
6	Root chord	150 mm
7	Tip chord	150 mm

3. THE AERODYNAMIC ANALYSIS OF THE UAV

Computational Fluid Dynamics (CFD) analysis can determine the airflow around the aircraft and how aerodynamic interference occurs. Therefore, for this analysis, two software systems have been chosen: XFLR5 and SolidWorks 2020. The first step to obtain the polar curves, in the XFLR5 software

system, is to establish the wing profiles (NACA 4412). The second step was to model the wing and finally to extract the results, i.e. the polar curves of the modelled wing (Figure 7). The distribution of the pressure coefficient at different angles of attack is depicted in the Figure 8.

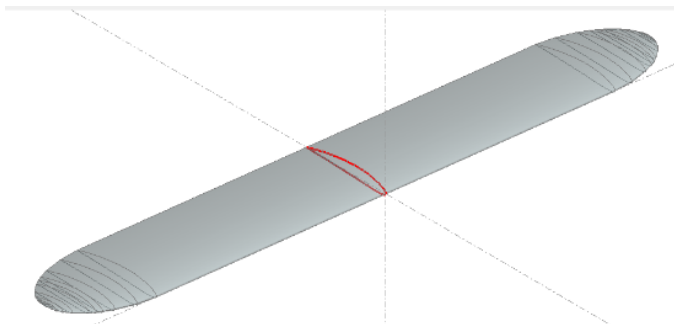


Figure 7. Wing modelling in XFLR5

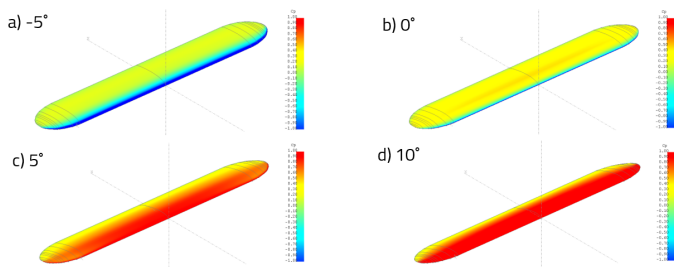


Figure 8. Variation of the pressure coefficient on the wing surface

After modelling the wing, its performance can be analysed. For the analysis the conditions of the aerodynamic analysis were set (speed is 10 m/s, and the range of angles of attack is -5 - 15 degrees). The results of the polar curve were shown in Figure 9.

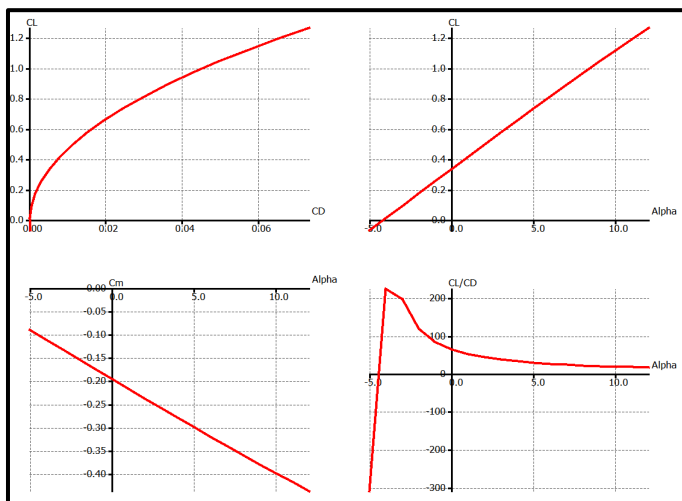


Figure 9. Polar curves of the airplane

Using the CFD module in SolidWorks and the 3D model of the aircraft, aerodynamic analysis was performed at 3 angles of attack. The results of the analysis for the aircraft at the three angles of attack are presented in Figure 10. As can be seen the highest pressure is located on the leading edge surface of the wing, but also on the empennage. There is also more evident pressure in the area of the

nose of the aircraft and the landing gear, especially the rear one. From the representation of the airfoils it can be seen that there is no aerodynamic interference between the wing structure and the empennage for any of the cases analysed, which confirms that the empennage designed in this form is advantageous.

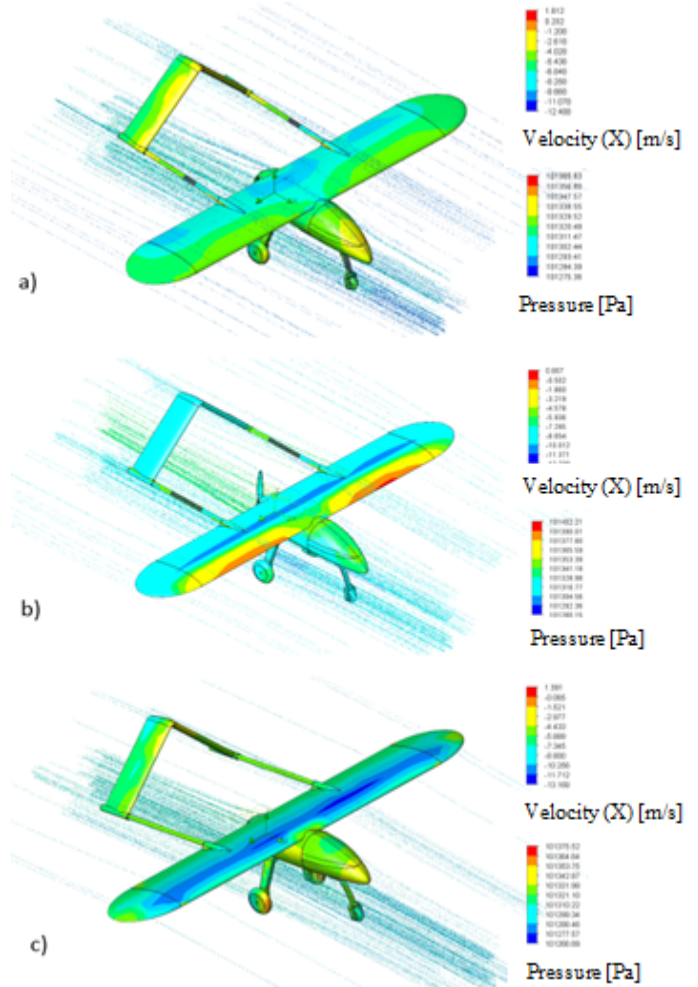


Figure 10. Aerodynamic analysis of the aircraft at three angles of attack of: a) -5°, b) 0°, c) 10°.

4. FINITE ELEMENT ANALYSIS

For the finite element analysis, the ANSYS 16 software system was chosen, using the structural static analysis module. The wing was fixed to the fuselage through these two screw holes and the area cut out specifically for the shape of the leading edge in the fuselage. The first step in the structural analysis of the wing is to establish the material used to manufacture the wing. For the PLA material the main material characteristics required for the FEA were introduced. The mesh contains elements of 2 mm in size. The next step determines the loadings acting on the wing. For this analysis two loadings are applied: load on the wing (wing weight x gravitational acceleration x safety factor); load on the empennage assembly (empennage weight x gravitational acceleration x safety factor).

As a result of the finite element analysis the following were determined: total deformations (Figure 11) and equivalent stresses (Figure 12). The maximum value of the equivalent stress (11.5 MPa) is lower than the allowable compressive strength (64.1 MPa) of the PLA from which the wing assembly is made, which confirms the strength of the structure to the applied loadings.

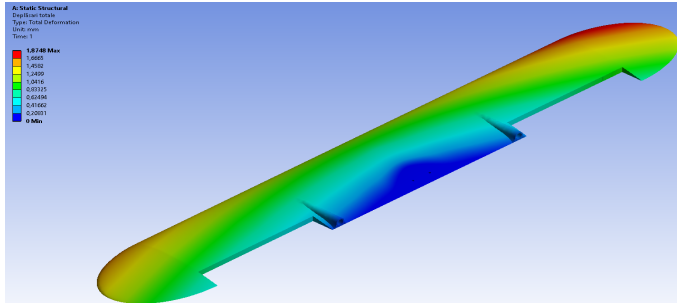


Figure 11. Total deformation

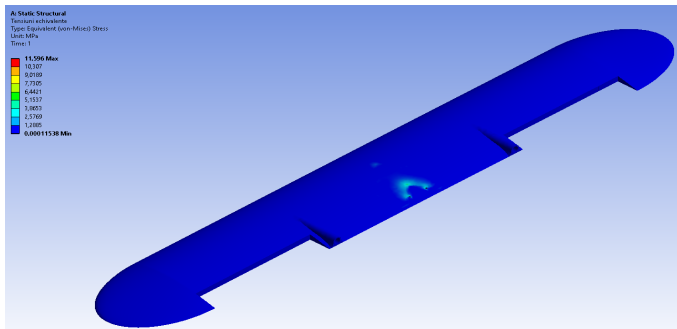


Figure 12. Equivalent stress

5. 3D PRINTING OF THE COMPONENTS

LW-PLA Gray Silver PLA filament was used to manufacture the aircraft components in order to obtain strong parts with low weight. The 3D printer used in this study was the Zortrax M300 Dual. The Z-Suite software system is used to make the code for the Zortrax printers. The manufacturing parameters for the aircraft components were described in Table 2. The way in which the aircraft components have been divided has been described in Figures 13,14,15 and 16.

Table 2. Manufacturing parameters of airplane components

Parameter	Value
Layer height [mm]	0.14
Infill density [%]	20
Printing speed [mm/sec]	50
Extrusion temperature [°C]	225
Bed Temperature [°C]	30
Nozzle diameter [mm]	0.4

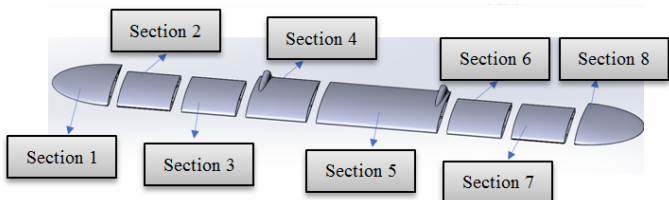


Figure 13. Wing sections

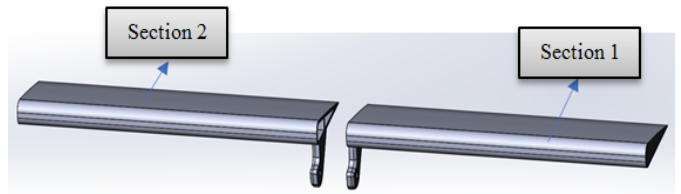


Figure 14. Control surfaces sections

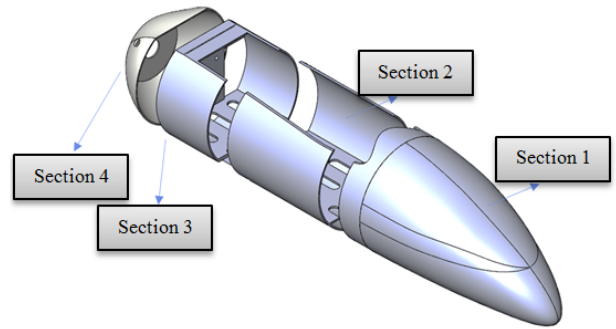


Figure 15. Fuselage sections

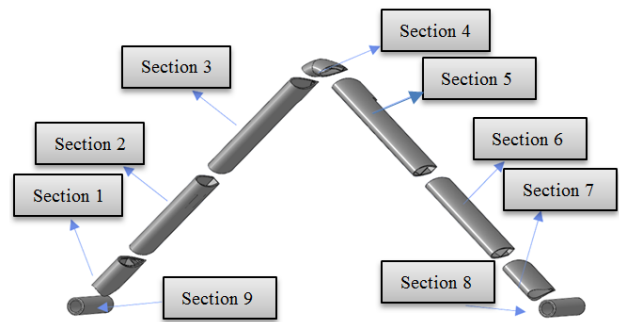


Figure 16. Vertical tail sections

Figures 17, 18 and 19 show some UAV components (wing sections, fuselage sections and main landing gear) manufactured by the FFF process. Table 3 details the manufacturing times of the UAV components.



Figure 17. 3D printing of wing sections

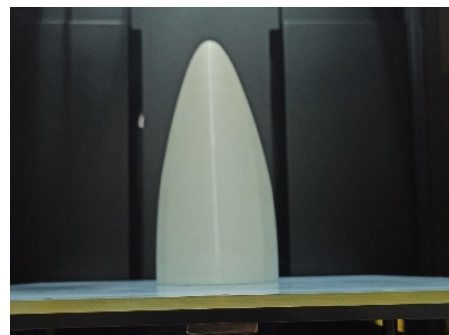


Figure 18. 3D printing of fuselage front section

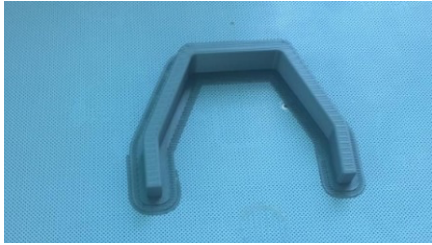


Figure 19. 3D printing of main landing gear

Table 3. 3D printing times of aircraft components

Component	3D printing time
Wing	3 days 2 hours and 43 minutes
Empennages	16 hours and 43 minutes
Fuselage	1 day 6 hours and 55 minutes
Control surfaces	13 hours and 58 minutes
Landing gear	17 hours and 50 minutes
Total	6 days and 10 hours and 9 minutes

6. ASSEMBLY OF THE AIRCRAFT COMPONENTS

After the completion of the sections, the assembly of the aircraft parts began: fuselage, wing, empennage, landing gear and electrical components. The servo controls were positioned in the sections of the fuselage, then the sections were bonded together to achieve the final shape (Figure 20). The brushless engine (Sunnysky Model X2814) was mounted on the designated area on the rear fuselage section (Figure 21). Then the propeller was mounted and the speed controller was installed (Figure 21).



Figure 20. Assembly of the vertical empennage

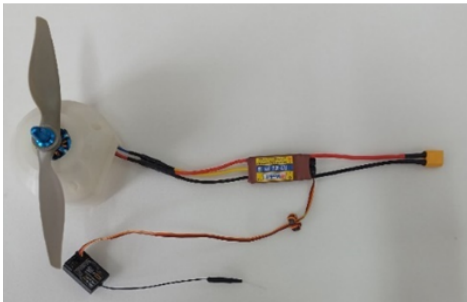


Figure 21. Assembly of the engine on the fuselage section

The fuselage sections (Figure 22) were bonded together with cyanoacrylate adhesive, the rear landing gear, and the rear fuselage assembly were then attached along with the engine. With the fuselage assembly the battery pack was also positioned.

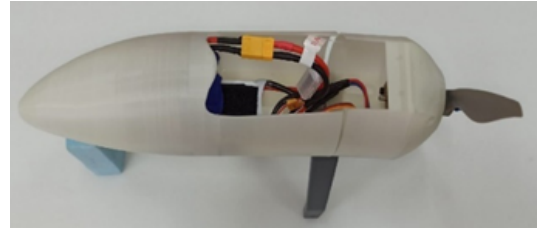


Figure 22. Assembling the fuselage

Next the servo controls were positioned in the slots provided for them in the wing sections, after which the sections were placed on the spar (carbon fibre pipe) to adjust its length (Figure 23).



Figure 23. Wing sections positioned on the spar

The wires from the servo controls were run to the power and control source (Figure 24). After the wires were connected, the attachment rods (made from carbon fibre) of the empennage were mounted and then secured in the designated areas on the wing.



Figure 24. Wing assembly - fixing rods – vertical empennage

The positioning of the control surfaces on the wing and the empennage was carried out using fibreglass strips (Figure 25).

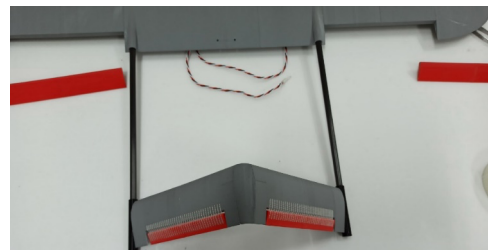


Figure 25. 3D printing of the main landing gear

The control surfaces were connected to the servomotor rods using bent rods, as shown in Figure 26.



Figure 26. Connecting the rod with the control surfaces

The wing - empennage assembly was attached to the fuselage using two screws located in the trailing edge area (Figure 27). The last stage consisted in fixing the camera holder and mounting the camera.



Figure 27. The UAV model manufactured by the FFF process

7. GROUND TESTING OF THE AIRCRAFT

The ground test checks the operation of the electrical systems, the engine and the control surfaces (servomotors that operate them). In the case of the controls on the empennage, due to its unconventional shape, it can be seen that they can move in the same direction but also in opposite directions (Figure 28). So if both are moved inwards or outwards during flight, the pitch angle will change, and if a surface is moved inwards and the other outwards will change the yaw angle. After the check was carried out it was concluded that all components, including the engine (Figure 29), were in good working order, ready for the first flight.

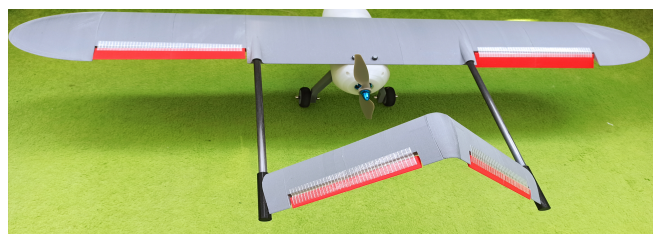


Figure 28. Checking the operation of the control surfaces



Figure 29. Checking the engine operation

8. CONCLUSIONS

After researching various innovative structural solutions, it is found that additive technology enables the actual manufacture of aircraft with components having complex surfaces. For the optimal manufacture of the UAV model, the thermoplastic filament extrusion process was used, using LW-PLA material, which has very good adhesion of the layers and is easy to manufacture. The manufacture of the UAV model using the thermoplastic filament extrusion process was not

difficult. Also, by using this material, lighter components with low density were obtained, due to the property of the material to turn into foam at a certain 3D printing temperature (about 225°C). In order to facilitate 3D printing, on the printer used, the components were sectioned into 32 sections, which were manufactured in 6 days, 10 hours and 9 min. In conclusion, it can be said that such an aircraft can be prepared for final assembly in a short time, without the need for moulds and complex manufacturing equipment. The UAV model can also be successfully used in surveillance, search - rescue missions using video cameras.

9. REFERENCES

1. Pascariu, I. S., Zaharia, S. M., Design and testing of an unmanned aerial vehicle manufactured by fused deposition modelling, *Journal of Aerospace Engineering*, Vol. 33, No.4, (2020).
2. Boukoberine, M. N., Zhou, Z., Benbouzid, M. A., Critical review on unmanned aerial vehicles power supply and energy management: Solutions, strategies, and prospects, *Applied Energy*, Vol. 255, (2019).
3. Hassanalian, M., Abdelkefi, A., Classifications, applications, and design challenges of drones: A review, *Progress in Aerospace Sciences*, Vol. 91, pp. 99-131, (2017).
4. Götten, F., Finger, D. F., Havermann, M., Braun, C., Marino, M., Bil, C., Full configuration drag estimation of short-to-medium range fixed-wing UAVs and its impact on initial sizing optimization, *CEAS Aeronautical Journal*, Vol 12, No. 3, pp. 589-603, (2021).
5. Skawiński, I., Goetzendorf-Grabowski, T. FDM 3D printing method utility assessment in small RC aircraft design, *Aircraft Engineering and Aerospace Technology*, Vol. 91, No.6, (2019).
6. Lancea, C., Chicos, L. A., Zaharia, S. M., Pop, M. A., Pascariu, I. S., Buican, G. R., Stamate, V. M. Simulation, Fabrication and Testing of UAV Composite Landing Gear, *Applied Sciences*, 12(17), (2022).
7. Kechagias, J., Chaidas, D., Vidakis, N., Salonitis, K., Vaxevanidis, N. M., Key parameters controlling surface quality and dimensional accuracy: A critical review of FFF process, *Materials and Manufacturing Processes*, Vol. 37, No. 9, pp. 963-984, (2022).
8. Anggraeni, D., Hidayat, D., Pramutadi, A. M., Rasyadi, A., Design and flight test of a medium range UAV for aerial photography, *International Journal of Unmanned Systems Engineering*, Vol. 3, No. 3, (2015).